J|A|C|S
ARTICLES
Published on Web 10/16/2004

Interfacial Electron-Transfer Kinetics of Ferrocene through Oligophenyleneethynylene Bridges Attached to Gold Electrodes as Constituents of Self-Assembled Monolayers: Observation of a Nonmonotonic Distance Dependence

John F. Smalley,*[,†,‡] Sandra B. Sachs,[§] Christopher E. D. Chidsey,[§] Stephen P. Dudek,[§] Hadley D. Sikes,[§] Stephen E. Creager,[||] C. J. Yu,[⊥] Stephen W. Feldberg,[†,‡] and Marshall D. Newton[‡]

Contribution from the Materials Science Department and Chemistry Department, Brookhaven National Laboratory, Upton, New York 11973-5000, Department of Chemistry, Stanford University, Stanford, California 94305-5080, Department of Chemistry, Clemson University, Clemson, South Carolina 29634, and Motorola Life Sciences, 757 South Raymond Avenue, Pasadena, California 91105

Received April 30, 2004; E-mail: smalley@bnl.gov

Abstract: The standard heterogeneous electron-transfer rate constants (k_n^0) between substrate gold electrodes and the ferrocene redox couple attached to the electrode surface by variable lengths of substituted or unsubstituted oligophenyleneethynylene (OPE) bridges as constituents of mixed self-assembled monolayers were measured as a function of temperature. The distance dependences of the unsubstituted OPE standard rate constants and of the preexponential factors (A_n) obtained from an Arrhenius analysis of the unsubstituted OPE k_n^0 versus temperature data are not monotonic. This surprising result, together with the distance dependence of the substituted OPE preexponential factors, may be assessed in terms of the likely conformational variability of the OPE bridges (as a result of the low intrinsic barrier to rotation of the phenylene rings in these bridges) and the associated sensitivity of the rate of electron transfer (and, hence, the single-molecule conductance which may be estimated using A_n) through these bridges to the conformation of the bridge. Additionally, the measured standard rate constants were independent of the identity of the diluent component of the mixed monolayer, and using an unsaturated OPE diluent has no effect on the rate of electron transfer through a long-chain alkanethiol bridge. These observations indicate that the diluent does not participate in the electron-transfer event.

Introduction

Over the past two decades, there has been a renewed interest in the study of the physical and chemical processes that control the kinetics of interfacial electron-transfer (ET) reactions. The scientific interest in these processes has been engendered by recent developments in a number of experimental techniques that have extended the range and utility of electrochemical kinetics measurements.[1,2] The kinetics of interfacial ET reactions are also important in a number of technological applications including those associated with biosensors,[3,4] photodiodes,[5,6] electrocatalysis,[7] bioelectrocatalysis,[8,9] solar photoconversion,[10] and, most especially, molecular electronics.[11−14]

A most convenient way to study the physical and chemical processes associated with interfacial ET is to measure the kinetics of electron-transfer reactions of redox moieties irreversibly attached to the surfaces of metal electrodes as a part of a stable, organized structure, that is, a self-assembled monolayer (SAM).[15−17] In such structures, the redox moiety is attached to

† Materials Science Department, Brookhaven National Laboratory.
‡ Chemistry Department, Brookhaven National Laboratory.
§ Stanford University.
|| Clemson University.
⊥ Motorola Life Sciences.

(1) Miller, C. J. In *Physical Electrochemistry, Principles, Methods and Applications*; Rubinstein, I., Ed.; Marcel Dekker: New York, 1995; pp 27−79.
(2) Feldberg, S. W.; Newton, M. D.; Smalley, J. F. In *Electroanalytical Chemistry*; Bard, A. J., Rubinstein, I., Eds.; Marcel Dekker: New York, 2003; Vol. 22, pp 101−180.
(3) Willner, I.; Heleg-Shabtai, V.; Blonder, R.; Katz, E.; Tao, G. L. *J. Am. Chem. Soc.* **1996**, *118*, 10321−10322.
(4) For recent examples, see: (a) Calvo, E. J.; Danilowicz, C.; Lagier, C. M.; Manrique, J.; Otero, M. *Biosensors and Bioelectronics* **2004**, *19*, 1219−1228. (b) Sen, S.; Gülce, A.; Gülce, H. *Biosens. Bioelectron.* **2004**, *19*, 1261−1268.
(5) Tang, C. W.; Vanslyke, S. A. *Appl. Phys. Lett.* **1987**, *51*, 913−915.
(6) (a) Burroughes, J. H.; Bradly, D. D. C.; Brown, A. R.; Marks, R. N.; Mackey, K.; Friend, R. H.; Burns, P. L.; Holmes, A. B. *Nature* **1990**, *347*, 539−541. (b) Ho, P. K. H.; Kim, J. S.; Burroughes, J. H.; Becker, H.; Li, S. F. Y.; Brown, T. M.; Cacialli, F.; Friend, R. H. *Nature* **2000**, *404*, 481−484. (c) Patel, N. K.; Cina, S.; Burroughes, J. H. *IEEE J. Quantum Electron.* **2002**, *8*, 346−361.
(7) (a) *Electrocatalysis*; Lipkowski, I., Ross, P. N., Eds.; John Wiley & Sons: New York, 1998; pp 1−400. (b) Valincius, G.; Niaura, G.; Kazakevičienė, B.; Talaikytė, Z.; Kažemėkaitė, M.; Butkus, E.; Razumas, V. *Langmuir* **2004**, *20*, 6631−6638.
(8) Hirsch, R.; Katz, E.; Willner, I. *J. Am. Chem. Soc.* **2000**, *122*, 12502−12504.
(9) Tsujimura, S.; Fujita, M.; Tatsumi, H.; Kano, K.; Ikeda, T. *Phys. Chem. Chem. Phys.* **2001**, *3*, 1331−1335.
(10) Anderson, N. A.; Ai, S.; Chen, D.; Mohler, D. L.; Lian, T. *J. Phys. Chem. B* **2003**, *107*, 14231−14239.
(11) Mirkin, C. A.; Ratner, M. A. *Annu. Rev. Phys. Chem.* **1992**, *92*, 719−754.
(12) Joachim, C.; Ginzewski, J. K.; Aviram, A. *Nature* **2000**, *408*, 541−548.

10.1021/ja047458b CCC: $27.50

the electrode as a component of a metallic electrode−bridge−redox couple arrangement[16] that corresponds to donor−spacer−acceptor structures which have been the subject of extensive investigations in homogeneous systems and biological structures.[1,18] Additionally, when a redox couple is attached to an electrode, a significant (surface) concentration of the couple can be located at a well-defined and variable distance from the electrode, the chemical composition of the bridge can also be varied, and complicating factors caused by diffusive and convective transport as well as by redox couple adsorption[17] are eliminated.

A number of studies from our and other laboratories have investigated the electron-transfer kinetics of both ferrocene[19−26] and pentaaminepyridine ruthenium[26−32] redox couples attached to Au electrodes through saturated alkane bridges as a function of the length (*l*) of the bridge. Some of us have also studied the electron-transfer kinetics of the ferrocene redox couple through unsaturated oligophenylenevinylene (OPV) bridges as a function of the length of the bridge.[33] The purpose of these studies was to characterize the role of both the length and the chemical composition of the bridge in mediating interfacial electron transfer. In the mixed self-assembled monolayer systems investigated in these studies (consisting of the redox moiety tethered to the electrode through the bridge and a diluent species also covalently attached to the surface of the electrode), both the standard ET rate constants (k_n^0) and the rate constant exponential decay coefficients ($\beta = -\mathrm{d}\ln[k_n^0]/\mathrm{d}l$) for the studied reactions were determined. Additionally, because Arrhenius preexponential factors contain information on the factors (other than those associated with the reorganization energy of the redox moiety) that determine the rate of an interfacial ET reaction (e.g., the electronic coupling if the ET reaction is nonadiabatic), we have also measured the standard ET rate constants of a variety of SAM component redox couple/bridge combinations[20,26,33] as a function of temperature. Arrhenius preexponential factors (A_n) were obtained from these measurements by fitting the k_n^0 versus temperature data to[26,33]

$$k_n^0 = A_n \exp[-E_{A,n}/RT] \quad (1)$$

where $E_{A,n}$ is the corresponding Arrhenius activation energy and the subscript "*n*" denotes that the relevant quantity is a function of the length (*l*) of the bridge (i.e., the bridge is an oligomer, and it contains *n* units of the pertinent monomer).

An important result demonstrated by these Arrhenius analyses[26,33] is that at short bridge lengths the preexponential factors limit at a surprisingly small value (much smaller than would be expected if, for example, the rate-determining step involved longitudinal relaxation dynamics of the aqueous solvent in contact with the SAMs) for both the alkane and the OPV bridges. Additionally, the alkane and OPV bridge A_n limits are different (the alkane limit being approximately 20 times smaller than the OPV limit).[26] One explanation for these observations is that, when A_n reaches a limiting value, the kinetics of the ET reaction are no longer controlled by the electronic coupling between the electrode and the redox moiety but by the kinetics of a slow change in the conformation of the bridge which accompanies the electron-transfer event.[26,33,34]

It has been shown by both density functional theory calculations[35] and generalized Mulliken−Hush calculations of electronic couplings[36] that the electron-transfer properties of oligophenyleneethynylene (OPE) bridges vary significantly depending on their molecular conformations. It has also been shown that the phenylene rings in OPE bridges have a low barrier to rotation,[35,37] which may result in an incomplete conjugation of these bridges that would, in turn, lower the rate of interfacial electron transfer through these bridges.[26] Additionally, comprehension of the mechanism of charge carrier transport in either single molecules or in small assemblies of molecules is most important for the design and construction of molecular-scale electronic devices. Because charge carrier transport should be extremely facile in π-conjugated materials such as OPEs,[38] electron (and hole) transport through systems based upon the aryleneethynylene architecture (substituted and unsubstituted OPEs) has been the subject of considerable recent study.[35,36,39−53] We, therefore, have employed the indirect laser-induced temperature jump (ILIT) technique[2] to measure the ET rate constants (k_n^0) of ferrocene attached (as a constituent of SAMs) to Au electrodes by various lengths of OPE bridges as a function of

(13) Adams, D. M.; Brus, L.; Chidsey, C. E. D.; Creager, S.; Creutz, C.; Kagan, C. R.; Kamat, P. V.; Lieberman, M.; Lindsay, S.; Marcus, R. A.; Metzger, R. M.; Michel-Beyerle, M. E.; Miller, J. R.; Newton, M. D.; Rolison, D. R.; Sankey, K. S.; Schanze, K. S.; Yardley, J.; Zhu, X. J. *J. Phys. Chem. B* **2003**, *107*, 6668−6697.
(14) Nitzan, A.; Ratner, M. A. *Science* **2003**, *300*, 1384−1389.
(15) Finklea, H. O. In *Electroanalytical Chemistry*; Bard, A. J., Rubinstein, I., Eds.; Marcel Dekker: New York, 1996; Vol. 19, pp 109−335.
(16) Newton, M. D.; Feldberg, S. W.; Smalley, J. F. In *Interfacial Electrochemistry, Theory, Experiment, and Applications*; Wieckowski, A., Ed.; Marcel Dekker: New York, 1999; pp 97−114.
(17) Smalley, J. F.; Geng, L.; Chen, A.; Feldberg, S. W.; Lewis, N. S.; Cali, G. *J. Electroanal. Chem.* **2003**, *549*, 13−24.
(18) (a) Wasielewski, M. R. *Chem. Rev.* **1992**, *92*, 435−461. (b) Winkler, J. R.; Gray, H. B. *Chem. Rev.* **1992**, *92*, 369−379.
(19) Chidsey, C. E. D. *Science* **1991**, *251*, 919−922.
(20) Smalley, J. F.; Feldberg, S. W.; Chidsey, C. E. D.; Linford, M. R.; Newton, M. D.; Liu, Y.-P. *J. Phys. Chem.* **1995**, *99*, 13141−13149.
(21) Weber, K.; Creager, S. E. *Anal. Chem.* **1994**, *66*, 3164−3172.
(22) Richardson, J. N.; Peck, S. R.; Curtin, L. S.; Tender, L. M.; Terrill, R. H.; Carter, M. T.; Murray, R. W.; Rowe, G. K.; Creager, S. E. *J. Phys. Chem.* **1995**, *99*, 766−772.
(23) Weber, K.; Hockett, L.; Creager, S. E. *J. Phys. Chem. B* **1997**, *101*, 8286−8291.
(24) Sumner, J. J.; Weber, K. S.; Hockett, L. A.; Creager, S. E. *J. Phys. Chem. B* **2000**, *104*, 7449−7454.
(25) Sumner, J. J.; Creager, S. E. *J. Am. Chem. Soc.* **2000**, *122*, 11914−11920.
(26) Smalley, J. F.; Finklea, H. O.; Chidsey, C. E. D.; Linford, M. R.; Creager, S. E.; Ferraris, J. P.; Chalfant, K.; Zawodzinski, T.; Feldberg, S. W.; Newton, M. D. *J. Am. Chem. Soc.* **2003**, *125*, 2004−2013.
(27) Finklea, H. O.; Hanshew, D. D. *J. Am. Chem. Soc.* **1992**, *114*, 3173−3181.
(28) Finklea, H. O.; Ravenscroft, M. S.; Snider, D. A. *Langmuir* **1993**, *9*, 223−227.
(29) Ravenscroft, M. S.; Finklea, H. O. *J. Phys. Chem.* **1994**, *98*, 3843−3850.
(30) Finklea, H. O.; Liu, L.; Ravenscroft, M. S.; Punturi, S. *J. Phys. Chem.* **1996**, *100*, 18852−18858.
(31) Finklea, H. O.; Ravenscroft, M. S. *Isr. J. Chem.* **1997**, *37*, 179−184.
(32) Brevnov, D. A.; Finklea, H. O.; VanRyswyk, H. *J. Electroanal. Chem.* **2001**, *500*, 100−107.
(33) Sikes, H. D.; Smalley, J. F.; Dudek, S. P.; Cook, A. R.; Newton, M. D.; Chidsey, C. E. D.; Feldberg, S. W. *Science* **2001**, *291*, 1519−1523.
(34) Bixon, M.; Jortner, J. *Russ. J. Electrochem.* **2003**, *39*, 3−8.
(35) Seminario, J. M.; Zacarias, A. G.; Tour, J. M. *J. Am. Chem. Soc.* **1998**, *120*, 3970−3974.
(36) Sachs, S. B.; Dudek, S. P.; Hsung, R. P.; Sita, L. R.; Smalley, J. F.; Newton, M. D.; Feldberg, S. W.; Chidsey, C. E. D. *J. Am. Chem. Soc.* **1997**, *119*, 10563−10564.
(37) Okuyama, K.; Hasegawa, T.; Ito, M.; Mikami, N. *J. Phys. Chem.* **1984**, *88*, 1711−1716.
(38) Walters, K. A.; Ley, K. D.; Cavalaheiro, C. S. P.; Miller, S. E.; Gosztola, D.; Wasielewski, M. R.; Bussandri, A. J.; vanWilligen, H.; Schanze, K. S. *J. Am. Chem. Soc.* **2001**, *123*, 8329−8342.
(39) Dhirani, A.; Lin, P.-H.; Guyot-Sionnest, P.; Zehner, R. W.; Sita, L. R. *J. Chem. Phys.* **1997**, *106*, 5249−5253.
(40) Chen, J.; Reed, M. A.; Rawlett, A. M.; Tour, J. M. *Science* **1999**, *286*, 1550−1552.
(41) Seminario, J. M.; Zacarias, A. G.; Tour, J. M. *J. Am. Chem. Soc.* **2000**, *122*, 3015−3020.
(42) Tour, J. M. *Acc. Chem. Res.* **2000**, *33*, 791−804.
(43) Reed, M. A.; Chen, J.; Rawlett, A. M.; Price, D. W.; Tour, J. M. *Appl. Phys. Lett.* **2001**, *78*, 3735−3737.

Chart 1

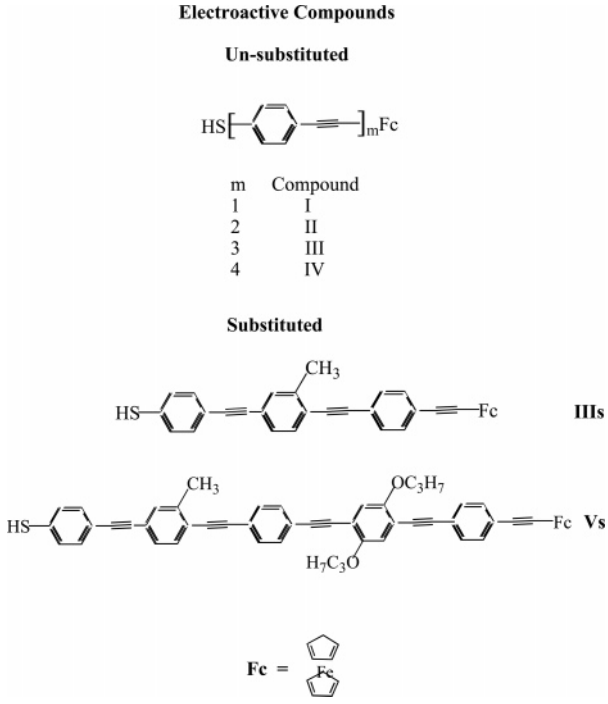

temperature to determine the distance dependence of A_n for this redox couple/bridge combination.[26]

The present paper expands upon our previous reports on the distance dependence of the interfacial electron-transfer rate constants of ferrocene through both substituted[53] and unsubstituted[36] OPE bridges at 298 K. We find that, contrary to the behavior we observed with alkane[20,26] and OPV[33] bridges, the distance dependence of the A_n determined here for the unsubstituted OPE bridges (see Chart 1) is not monotonic. We also find that the addition of substituents on the OPE bridge has a significant effect on A_n (and, consequently, on the rate of electron transfer through the bridge). Because of the conformational flexibility of OPE bridges, we argue that these observations are consistent with the suggestion (made before for alkane[26] and OPV[33] bridges) that the rate of electron transfer through the OPE bridges is influenced by dispersion in the conformations of the bridge.[34] We also demonstrate that the diluent constituents of the mixed SAMs investigated in the present and previous studies[2,15] of the ET kinetics of attached redox couples do not participate in the electron-transfer event, and we will demonstrate how the results of the present study may be used[13,26] to estimate the single-molecule conductivities of OPE bridges.

Chart 2.[a]

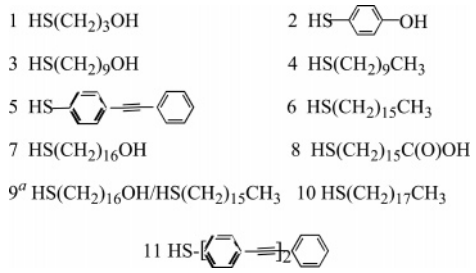

[a] The electrode preparation solutions contained equal concentrations of these diluents.

Experimental Section

Materials and Methods. The syntheses of the unsubstituted electroactive OPE thiols (Chart 1) and their thioacetates as well as diluent 5 (Chart 2) are described in refs 54 and 55. ^{1}H NMR (200 to 500 MHz)[54a,55] as well as both low- and high-resolution mass spectrometry[54a] were used to characterize these unsubstituted compounds. The syntheses of the substituted OPE electroactive compounds (Chart 1) are described in ref 56. ^{1}H NMR (300 MHz) and high-resolution mass spectrometry were also used to characterize these substituted compounds.[56] Descriptions of the syntheses and characterizations of diluents 3, 7, and 8 (Chart 2) may be found in ref 57. The characterizations establish that all of the electroactive compounds in Chart 1 are highly pure.

The ~1 μm thick gold film working electrodes used in the present study were vapor deposited[2] over 500 Å thick layers of titanium vapor deposited on quartz disks so that the microcrystallites comprising the front surfaces of these electrodes have a uniform 111 orientation.[20] Mixed monolayers of the unsubstituted electroactive thiols were prepared by placing a cleaned gold film electrode into a chloroform solution containing a mixture of the electroactive compound (Chart 1) and the relevant diluent thiol (Chart 2). The total concentration of thiol in these coating solutions was approximately 5.0×10^{-4} M, and the mole fraction of the electroactive thiol was varied to give different concentrations of the redox couple in the monolayer. The electrodes remained in these coating solutions for approximately 16 h (overnight), were rinsed in a succession of chloroform, *n*-hexane, water, and chloroform, were dried in a stream of argon, and were attached to the ILIT cell containing the aqueous electrolyte solution.

(44) (a) Fan, F.-R. F.; Yang, J.; Cai, L.; Price, D. W., Jr.; Dirk, S. M.; Kosynkin, D. V.; Yao, Y.; Rawlett, A. M.; Tour, J. M.; Bard, A. J. *J. Am. Chem. Soc.* **2002**, *124*, 5550−5560. (b) Fan, F.-R.; Lai, R. Y.; Cornil, J.; Karzazi, Y.; Brédas, J.-L.; Cai, L.; Cheng, L.; Yao, Y.; Price, D. W., Jr.; Dirk, S.: Tour, J. M.; Bard, A. J. *J. Am. Chem. Soc.* **2004**, *126*, 2568−2573. (c) Fan, F.-R.; Yao, Y.; Cai, L.; Cheng, L.; Tour, J. M.; Bard, A. J. *J. Am. Chem. Soc.* **2004**, *126*, 4035−4042.
(45) Rawlett, A. M.; Hopson, T. J.; Nagahara, L. A.; Tsui, R. K.; Ramachandran, G. K.; Lindsay, S. M. *Appl. Phys. Lett.* **2002**, *81*, 3043−3045.
(46) Ramachandran, G. K.; Hopson, T. J.; Rawlett, A. M.; Nagahara, L. A.; Primak, A.; Lindsay, S. M. *Science* **2003**, *300*, 1413−1416.
(47) (a) Dunbar, T. D.; Cygan, M. T.; Bumm, L. A.; McCarty, G. S.; Burgin, T. P.; Reinerth, W. A.; Jones, L., II; Jackiw, J. J.; Tour, J. M.; Weiss, P. S.; Allara, D. L. *J. Phys. Chem. B* **2000**, *104*, 4880−4893. (b) Donhauser, Z. L.; Mantooth, B. A.; Kelly, K. F.; Bumm, L. A.; Monnell, J. D.; Stapleton, J. J.; Price, D. W., Jr.; Rawlett, A. M.; Allara, D. L.; Tour, J. M.; Weiss, P. S. *Science* **2001**, *292*, 2303−2307. (c) Lewis, P. A.; Donhauser, Z. J.; Mantooth, B. A.; Smith, R. K.; Bumm, L. A.; Kelly, K. F.; Weiss, P. S. *Nanotechnology* **2001**, *12*, 231−237. (d) Donhauser, Z. J.; Mantooth, B. A.; Pearl, T. P.; Kelly, K. F.; Nanayakkara, S. U.; Weiss, P. S. *Jpn. J. Appl. Phys.* **2002**, *41*, 4871−4877.
(48) Weber, H. B.; Reichert, J.; Weigend, F.; Ochs, R.; Beckmann, D.; Mayor, M.; Ahlrichs, R.; Löhneysen, H. v. *Chem. Phys.* **2002**, *281*, 113−125.
(49) (a) Kushmerick, J. G.; Holt, D. B.; Pollack, S. K.; Ratner, M. A.; Yang, J. C.; Schull, T. L.; Naciri, J.; Moore, M. H.; Shashidhar, R. *J. Am. Chem. Soc.* **2002**, *124*, 10654−10655. (b) Cai, L. T.; Skulason, H.; Kushmerick, J. G.; Pollack, S. K.; Naciri, J.; Shashidhar, R.; Allara, D. L.; Mallouk, T. E.; Mayer, T. S. *J. Phys. Chem. B* **2004**, *108*, 2827−2832.
(50) Cornil, J.; Karzazi, Y.; Brédas, J. L. *J. Am. Chem. Soc.* **2002**, *124*, 3516−3517.
(51) Walzer, K.; Marx, E.; Greenham, N. C.; Less, R. J.; Raithby, P. R.; Stokbro, K. *J. Am. Chem. Soc.* **2004**, *126*, 1229−1234.
(52) Selzer, Y.; Cabassi, M. A.; Mayer, T. S.; Allara, D. L. *J. Am. Chem. Soc.* **2004**, *126*, 4052−4053.
(53) Creager, S. E.; Yu, C. J.; Bamdad, C.; O'Connor, S.; MacLean, T.; Lam, E.; Chong, Y.; Olsen, G. T.; Luo, J.; Gozin, M.; Kayyem, J. F. *J. Am. Chem. Soc.* **1999**, *121*, 1059−1064.
(54) (a) Hsung, R. P.; Chidsey, C. E. D.; Sita, L. R. *Organometallics* **1995**, *14*, 4808−4815. (b) Dhirani, A. A.; Zehner, R. W.; Hsung, R. P.; Guyot-Sionnest, P.; Sita, L. R. *J. Am. Chem. Soc.* **1996**, *118*, 3319−3320.
(55) Sachs, S. B. Ph.D. Thesis, Stanford University, Stanford, CA, 2000.
(56) Yu, C. J.; Chong, Y.; Kayyem, J. F.; Gozin, M. *J. Org. Chem.* **1999**, *64*, 2070−2079.
(57) Bain, C. D.; Troughton, E. B.; Tao, Y.-T.; Evall, J.; Whitesides, G. M.; Nuzzo, R. G. *J. Am. Chem. Soc.* **1989**, *111*, 321−335. See the Supporting Information accompanying this reference for the synthetic and characterization procedures for these diluents.

In some cases, the unsubstituted electroactive OPE compound was protected by a thioacetate group. These protected compounds were deprotected by adding ~0.4 M of diethylamine to the electrode coating solution described in the preceding paragraph and mildly heating the resulting solution under argon at 50 °C for approximately 24 h. A cleaned electrode was placed in the "deprotected" coating solution, and the monolayer deposition was accomplished (over 16 h) under an argon atmosphere. The method of preparation of the mixed monolayers containing the electroactive unsubstituted OPE compounds has no effect upon the results observed in the present study.[58]

The terminal thiol groups of the substituted electroactive OPE compounds were initially protected by 4-ethyl-*N*-methylpyridinium iodide (Chart 1). Stock solutions of the deprotected, substituted electroactive compounds were prepared by placing a small amount of the protected compound into a 9:1 ethanol:triethylamine solution (the concentration of the electroactive compounds in these solutions was $\sim 2.5 \times 10^{-4}$ M) for at least 10 min at room temperature.[53] These stock solutions were stored in capped polypropylene vials in a freezer. A mixed monolayer containing a deprotected, substituted compound was prepared by placing a cleaned gold film electrode into an ethanol solution (coating solution) containing an aliquot of one of these stock solutions mixed with the appropriate diluent thiol for ~24 h. The total concentration of thiol in this first coating solution was $\sim 2.5 \times 10^{-4}$ M, and, as before, the mole fraction of electroactive thiol was varied to give different concentrations of the redox couple in the monolayer. After the initial deposition of the mixed monolayer, the electrode was removed from the first coating solution, rinsed in ethanol, and placed into a second coating solution containing 1.0×10^{-3} M of the relevant diluent thiol for ~16 h. The electrode was then removed from this second coating solution, briefly rinsed in ethanol, quickly dried in a stream of argon, and attached to the ILIT cell.

Aldrich alkanethiols (Chart 2), Aaper absolute ethyl alcohol, Baker Ultrex ultrapure $HClO_4$, Aldrich spectrophotometric grade chloroform, Aldrich anhydrous *n*-hexane, Johnson Matthey 99% pure (metals basis) $NaClO_4 \cdot H_2O$, Aldrich 4-mercaptophenol, and Fisher reagent grade diethylamine and triethylamine were all used as received. Except for a single ILIT experiment where the aqueous electrolyte solution was 1.0 M $NaClO_4$, this solution was always 1.0 M $HClO_4$. The water used to make these electrolyte solutions was purified in a Millipore Mill-Q Plus system. The gold film electrodes employed in this study were cleaned in an argon ion plasma before use. Cyclic voltammograms (CVs) of the SAMs investigated in this work were taken before each ILIT experiment on a BAS 100BW electrochemical analyzer, and a saturated sodium calomel reference electrode (SSCE) was used in all experiments.

The ILIT Technique and Data Analysis. The ILIT apparatus, cell, and experimental techniques have all been fully described elsewhere.[2,20,59,60] The open circuit potential transients resulting from the (2−5 °C) ILIT temperature perturbations were fitted to[2,20,60]

$$\Delta V(t) = A'\Delta T^*(t) + B'k_m(E_i)\int_0^t \exp[-k_m(E_i)(t-\tau)]\Delta T^*(t)\,d\tau \quad (2)$$

where $\Delta V(t)$ is the change in the open circuit potential at time t, A' is the amplitude of the (initial) thermal response, B' is the amplitude of the electron-transfer relaxation, and $k_m(E_i)$ is the measured (experimental) rate constant (s^{-1}) for this relaxation at the initial (applied) potential (E_i). ΔT^* (t and τ) in eq 2 is the convolution of the temperature perturbation at the electrode/electrolyte interface and the instrument response function divided by the interfacial temperature change (ΔT_{eq}) that would be produced if all of the absorbed heat were uniformly distributed in the electrode and none of this heat were lost to either the quartz disk or the electrolyte solution.[2,20,60] Standard electron-transfer rate constants (k_n^0, the rate constant at the formal potential ($E^{o\prime}$) of the redox couple) were obtained from fits of the plots of $k_m(E_i)$ versus E_i to[61]

$$k_m(E_i) = \frac{k_n^0\gamma\omega(E_i)^{1/2}}{1+\omega(E_i)}\left\{1 + \frac{[1+\omega(E_i)]^2}{\gamma\omega(E_i)}\right\} \quad (3)$$

where

$$\gamma = N_T F^2/RTC_{film} \quad (4)$$

and

$$\omega(E_i) = \exp[(F/RT)(E_i - E^{o\prime})] \quad (5)$$

In eqs 4 and 5, F is the Faraday constant, R is the ideal gas constant, T is the absolute temperature, N_T is the number of redox species attached to the electrode (mol), and C_{film} is the double layer capacitance of the electrode/electrolyte solution interface (F). Values of γ and $E^{o\prime}$ may be derived from either the fit of $k_m(E_i)$ versus E_i to eqs 3 and 5 or the cyclic voltammogram for a SAM containing the attached ferrocene redox couple.

As we have done before,[26,33] to accomplish a simple and consistent analysis of the temperature dependence of k_n^0 without having to presume a mechanism for the electron-transfer event,[62] these data were fitted to eq 1. If, for example, the electron transfer proceeds by a coherent tunneling process (i.e., by a superexchange mechanism[63] and the interfacial electron-transfer reaction is nonadiabatic), the Arrhenius preexponential factor and activation energy are well approximated by[20,26,64]

$$A_{n,NA} = 2\pi^{3/2}H_{ab,n}{}^2\rho_m/h \quad (6)$$

and

$$E_{A,n,NA} = \lambda_n/4 \quad (7)$$

where the subscript "NA" specifically identifies these quantities for a nonadiabatic reaction, $H_{ab,n}$ is the electronic coupling between the electrode and the redox moiety through a bridge whose length is defined by the subscript "n", ρ_m is the density of electronic states in the metal electrode, h is Planck's constant, and λ_n is the reorganization energy for the electron-transfer reaction.

Results and Discussion

ILIT Measurements of Interfacial ET Standard Rate Constants. Figure 1 shows cyclic voltammograms for two mixed monolayers composed of the electroactive compounds IV and IIIs (see Chart 1) mixed with the alkanethiol diluents 10 and 6 (see Chart 2), respectively. An example of the cyclic voltammograms observed when an ω-hydroxythiol was the diluent is shown in Figure 3 of ref 61. The cyclic voltammograms shown in Figures 1 and 3 of ref 61 are representative of all those observed in the present study,[21] and they demonstrate that the monolayers made in the present study are all densely packed and contain a minority component of isolated and

(58) Stapleton, J. J.; Harder, P.; Daniel, T. A.; Reinard, M. D.; Yao, Y.; Price, D. W.; Tour, J. M.; Allara, D. L. *Langmuir* **2003**, *19*, 8245−8255.
(59) Smalley, J. F.; Krishnan, C. V.; Goldman, M.; Feldberg, S. W.; Ruzic, I. *J. Electroanal. Chem.* **1988**, *248*, 255−282.
(60) Smalley, J. F.; Geng, L.; Feldberg, S. W.; Rogers, L. C.; Leddy, J. *J. Electroanal. Chem.* **1993**, *356*, 181−200.
(61) Smalley, J. F.; Newton, M. D.; Feldberg, S. W. *Electrochem. Commun.* **2000**, *2*, 832−838.
(62) Forster, R. J.; Loughman, P.; Keyes, T. E. *J. Am. Chem. Soc.* **2000**, *122*, 11948−11955.
(63) McConnell, H. M. *J. Chem. Phys.* **1961**, *35*, 508−515.
(64) (a) Marcus, R. A. *J. Chem. Phys.* **1965**, *43*, 679−701. (b) For simplicity, the definition of $A_{n,NA}$ in eq 6 omits a factor of order unity.[20,26]

Table 1. Standard Electron-Transfer Rate Constants (k_n^0) at $T = 25$ °C, Activation Energies ($E_{A,n}$), Reorganization Energies ($\lambda_{n,app}$),[66] and Arrhenius Preexponential Factors (A_n) Measured Using ILIT for Mixed Monolayers Containing the Electroactive OPE Compounds (See Chart 1)

bridge[a]	l[b]/Å	diluents[c] (E°/mV vs SSCE)[d]	k_n^0[e]/s^{-1}	$E_{A,n}$[e,f]/eV	$\lambda_{n,app}$[e,g]/eV	ln[A_n/s^{-1}][e]
I	6.9	1 (310) 2 (298)	$(1.5 \pm 0.1) \times 10^7$	0.18 ± 0.01	0.72 ± 0.04	23.48 ± 0.59
II[h]	13.8	3 (308) 4 (376) 5 (339)	$(3.3 \pm 0.2) \times 10^6$	0.27 ± 0.01	1.09 ± 0.05	25.63 ± 0.60
III[h]	20.7	6 (346) 7 (342) 8 (315) 9 (349)	$(6.4 \pm 0.4) \times 10^4$	$0.27 \pm 0.01_5$	1.06 ± 0.06	21.36 ± 0.62
IV	27.5	6 (350) 10 (378)	$(1.2 \pm 0.1) \times 10^5$	0.28 ± 0.01	1.11 ± 0.03	22.50 ± 0.54
IIIs	20.7	6 (387) 7 (350,335[i])	$(2.3 \pm 0.2) \times 10^6$	0.25 ± 0.01	0.99 ± 0.05	24.29 ± 0.62
Vs	34.4	7 (351)	$(3.1 \pm 0.2) \times 10^4$	0.25 ± 0.01	0.99 ± 0.03	19.94 ± 0.56

[a] Bridges of the electroactive compounds described in Chart 1 where the subscript "n" refers to the number of phenyleneethynylene (PE) units in the bridge. [b] l is the straight-line distance from the bridge carbon attached to the sulfur to the attached carbon of the cyclopentadiene ring of the ferrocene ($l = 0$ when the cyclopentadiene carbon is attached to the sulfur) based on mean bond distances.[54] [c] Diluents described in Chart 2. [d] In this column, the numbers in parentheses are the average formal potentials ($E^{\circ\prime}$) observed in the cyclic voltammograms with the respective diluents. [e] For each bridge, the average of all of the k_n^0's obtained from measurements on mixed monolayers made from all of the diluents listed in the third column of this table. The values of $E_{A,n}$ and ln[A_n] are obtained from linear least-squares fits to the data plotted in Figure 6. The errors for all of these data are at the 2σ limit. [f] Arrhenius activation energy (see the text). [g] Reorganization energy obtained from the Arrhenius analysis[66] calculated as $\lambda_{n,app} = 4E_{A,n}$ (see the text). [h] Including k_n^0 data reported in ref 36. [i] 1.0 M $NaClO_4$ electrolyte solution.

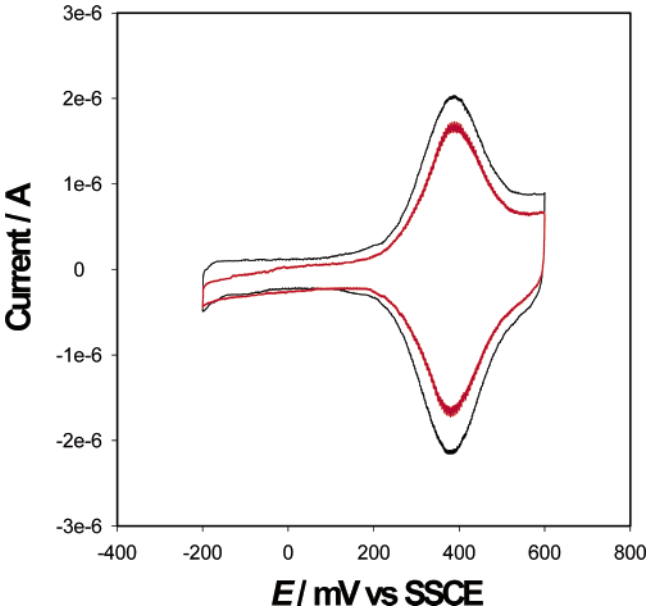

Figure 1. Cyclic voltammograms of mixed monolayers containing electroactive compounds IV and IIIs (see Chart 1). Black line: compound IV, $HS(CH_2)_{17}CH_3$ diluent (number 10 in Chart 2), $T = 24$ °C, $FN_T = 2.48 \times 10^{-6}$ C (see eq 4). Red line: compound IIIs, $HS(CH_2)_{15}CH_3$ diluent (number 6 in Chart 2), $T = 23$ °C, $FN_T = 1.93 \times 10^{-6}$ C (see eq 4).

identical redox moieties.[65] The average formal potentials ($E^{\circ\prime}$) of the ferrocene redox couple are given in parentheses in the third column of Table 1. The experimental error for all of the formal potentials reported in Table 1 is ±10 mV. The measured ferrocene redox couple formal potentials for mixed monolayers where the diluent is terminated by a polar functional group are somewhat less positive than those measured for mixed monolayers where the diluent is terminated by a methyl group. However, for a particular electroactive compound, the measured value of k_n^0 is immune to these differences in $E^{\circ\prime}$ and the consequent small differences in the thermodynamic properties of the interfacial electron-transfer reaction (see Figures 2 and 14 in ref 2). The average full-width at half-maximum (fwhm) of all of the cyclic voltammograms measured in the present study is (123 ± 11) mV. As we have previously observed for other types of bridges, this value of fwhm is close to[33] but a little larger[26] than the theoretically expected value of 91 mV at 25 °C.

Examples of the open circuit (ILIT) responses observed in this work are shown in Figures 2 and 3. Both of the ILIT responses in Figure 2 were measured at a potential within ±10 mV of the relevant $E^{\circ\prime}$. The most important thing to note about the ILIT data shown in Figures 2 and 3 is that these transient responses are well fit by eq 2 as are all of the ILIT responses observed in the present study. Figure 4 demonstrates that values of $k_m(E_i)$ (see eq 2) measured as a function of E_i are well fit by eqs 3−5. Evalutions of γ and $E^{\circ\prime}$ obtained from fits such as those shown in Figure 4 are very close (typically within ±10% for γ and ±10 mV for $E^{\circ\prime}$) to the values obtained from the cyclic voltammograms.[61] This equivalence of the values of γ determined by cyclic voltammetry and ILIT means that both techniques are sampling the same populations of the ferrocene redox couple.[61] Furthermore, the measured rate constants are always well fit by the potential dependence defined by eqs 3−5, and the standard rate constants obtained from these fits are always independent of N_T (i.e., the concentration of the redox moiety in the mixed monolayer; see Figure 4). These observations confirm that the behavior of the ILIT transient is, in fact, effected by an electron-transfer relaxation. It should also be noted that, because the ILIT response is a change in the open circuit potential, it is unaffected by uncompensated solution resistance.[2,26]

The fourth column of Table 1 gives the standard rate constants (k_n^0) at 25 °C for all of the substituted and unsubstituted OPE

(65) Chidsey, C. E. D.; Bertozzi, C. R.; Putvinski, T. M.; Mujsce, A. M. *J. Am. Chem. Soc.* **1990**, *112*, 4301−4306. See Figure 2 in this reference for examples of cyclic voltammograms of mixed alkanethiol SAMs in which the ferrocene redox moieties are not isolated and, therefore, not identical.

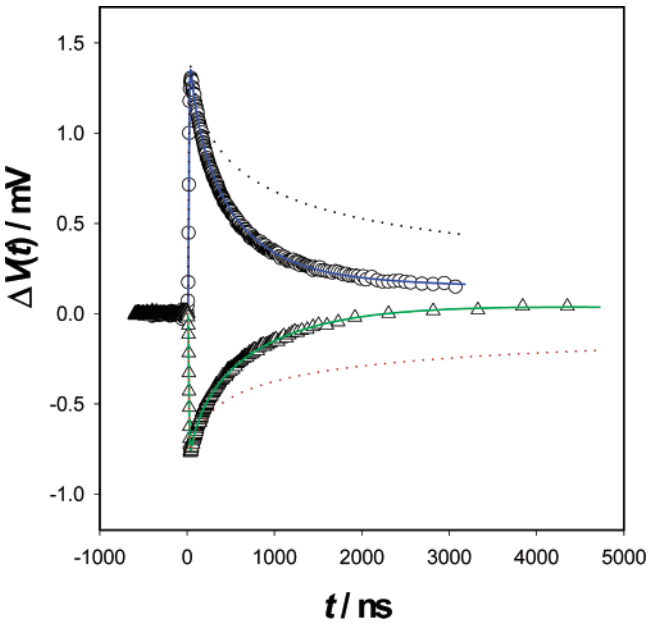

Figure 2. ILIT responses (at initial $T = 25.2$ °C) from Au electrodes coated with mixed monolayers containing either electroactive compound IV or Vs. ○: mixed monolayer composed of electroactive compound IV and HS-$(CH_2)_{15}CH_3$ (diluent 6 in Chart 2) at $E_i = 350$mV vs SSCE. The blue solid line through these points describes a fit of these data to eq 2, resulting in $A' = 1.7$ mV, $B' = -0.94$ mV, and $k_m(E_i) = 1.4 \times 10^6$ s^{-1}. △: mixed monolayer composed of electroactive compound Vs and HS$(CH_2)_{16}$OH (diluent 7 in Chart 2) at $E_i = 350$ mV vs SSCE. The green solid line through these points describes a fit of these data to eq 2, resulting in $A' = -0.94$ mV, $B' = 0.96$ mV, and $k_m(E_i) = 6.3 \times 10^5$ s^{-1}. The black and red dotted lines represent the responses that would be observed if there were no relaxation of the ILIT signal caused by electron transfer between the electrodes and the ferrocene redox couple for the signals described by ○ and △, respectively.

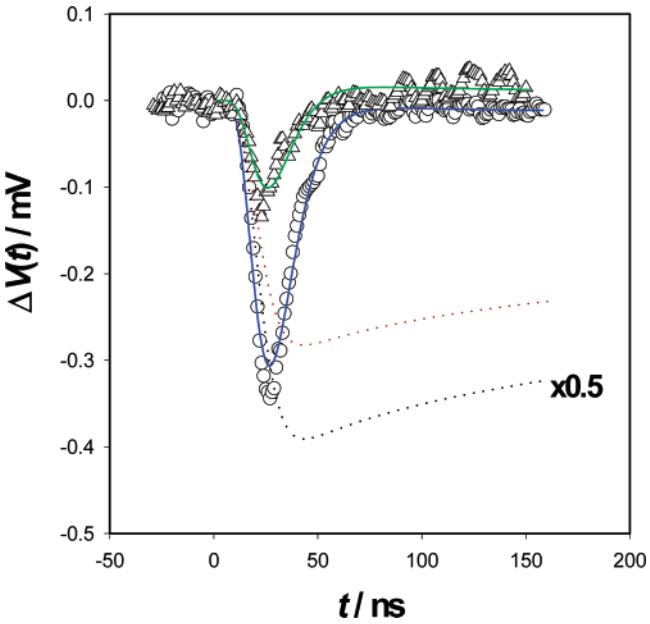

Figure 3. ILIT responses from Au electrodes coated with mixed monolayers containing either electroactive compound I or IIIs. ○: mixed monolayer composed of electroactive compound IIIs and HS$(CH_2)_{16}$OH (diluent 7 in Chart 2) at initial $T = 34.9$ °C and at $E_i = 400$ mV vs SSCE. The blue solid line through these points describes a fit of these data to eq 2, resulting in $A' = -0.95$ mV, $B' = 0.92$ mV, and $k_m(E_i) = 1.0 \times 10^8$ s^{-1}. △: mixed monolayer composed of electroactive compound I and 4-mercaptophenol (diluent 2 in Chart 2) at initial $T = 14.8$ °C and at $E_i = 350$ mV vs SSCE. The green solid line through these points describes a fit of these data to eq 2, resulting in $A' = -0.34$ mV, $B' = 0.36$ mV, and $k_m(E_i) = 1.1 \times 10^8$ s^{-1}. The black and red dotted lines represent the responses that would be observed if there were no relaxation of the ILIT signal caused by electron transfer between the electrodes and the ferrocene redox couple for the signals described by ○ and △, respectively. The black dotted line has been multiplied by 0.5.

electroactive compounds investigated in the present study. The values of k_n^0 (at 25 °C) reported in the fourth column of Table 1 are simply averages of all of the determinations for a particular bridge (electroactive compound; see footnote *e* in Table 1). We emphasize that the chemical identity of the diluent (or the length of the alkyl chain for an alkanethiol diluent) in the mixed monolayer used to determine the standard rate constant has no effect on the measured value of k_n^0 (or the measured activation energy ($E_{A,n}$) and Arrhenius preexponential factor (A_n); see below). Changing the electrolyte solution from 1.0 M $HClO_4$ to 1.0 M $NaClO_4$[53] also has no effect on k_n^0 (or $E_{A,n}$ and A_n). We also emphasize that the several diagnostic checks performed on the ILIT measurements of k_n^0 (such as determining the behavior of $k_m(E_i)$ as a function of potential (Figure 4), establishing that all of the ILIT measured k_n^0 are independent of N_T and verifying that, for each monolayer used to measure a k_n^0, the γ determined using ILIT and the γ measured using cyclic voltammetry are the same) confirm that these measurements are accurate.[68]

Figure 5 shows a plot of $\ln[k_n^0]$ (determined at 25 °C using both ILIT (on both substituted and unsubstituted electroactive compounds) and an ac voltammetry technique[69] (on substituted electroactive compounds alone[53])) versus l, where l is the shortest distance between the bridge carbon attached to the sulfur and the attached carbon of the ferrocene redox couple (see footnote *b* in Table 1). As before,[26] this definition of l, although a sensible choice, is entirely arbitrary. In general, k_n^0 decreases as the length of the bridge (l) increases, which suggests the anticipated (if the rate of electron transfer is controlled by a superexchange (tunneling) mechanism) decrease in the electronic coupling ($H_{ab,n}$) between the ferrocene redox moiety and the Au electrode as l increases. However, no attempt will be made to fit the data in Figure 5 to a theoretical expression because the bridge length dependence of these data is not entirely monotonic. For example, the k_n^0 for electroactive compound IV is larger than that measured for electroactive compound III despite the fact that l for compound IV is larger than l for compound III. Also, for bridges containing three phenyleneethynylene (PE) units, the standard rate constants for the substituted electroactive compound (IIIs in Chart 1, measured using both ILIT and ac voltammetry[53]) are much larger than that for the unsubstituted electroactive compound (III in Chart 1, measured using ILIT alone). We will discuss differences between the behaviors of substituted and unsubstituted electroactive compounds later. For the present, we note that the standard rate constants for the substituted electroactive compounds (IIIs and Vs in Chart 1) measured using ILIT are as much as a factor of 6 larger than those measured using ac voltammetry. Aside from the method of measurement, there are

(66) This is "apparent" because, for example, large electronic couplings ($H_{ab,n}$) can significantly lower $E_{A,n}$ (see eq 10 in ref 26).[67]
(67) (a) Brunschwig, B. S.; Sutin, N. *Coord. Chem. Rev.* **1999**, *187*, 233−254. (b) Sutin, N. *Prog. Inorg. Chem.* **1983**, *30*, 441−498.
(68) In agreement with the CV results discussed previously, these diagnostic checks also confirm that the ferrocene redox moieties are identical and isolated.
(69) Creager, S. E.; Wooster, T. T. *Anal. Chem.* **1998**, *70*, 4257−4263.

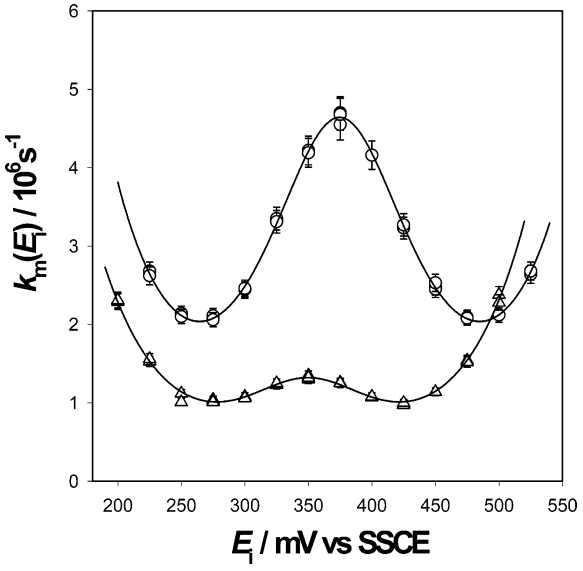

Figure 4. $k_m(E_i)$ as a function of E_i obtained from ILIT responses (at initial $T = 25.2$ °C) of Au electrodes coated with mixed monolayers containing electroactive compound IV. ○: $HS(CH_2)_{17}CH_3$ diluent (number 10 in Chart 2), the solid line through these points is the fit of these data to eqs 3 and 5, resulting in $E^{\circ\prime} = 375$ mV vs SSCE, $\gamma = 75$ (see eq 4; the γ calculated from the cyclic voltammogram of this monolayer is 74), and $k_n^0 = 1.2 \times 10^5$ s^{-1}. △: $HS(CH_2)_{15}CH_3$ diluent (number 6 in Chart 2), the solid line through these points is the fit of these data to eqs 3 and 5, resulting in $E^{\circ\prime} = 350$ mV vs SSCE, $\gamma = 18$ (see eq 4; the γ calculated from the cyclic voltammogram of this monolayer is also 18), and $k_n^0 = 1.2 \times 10^5$ s^{-1}.

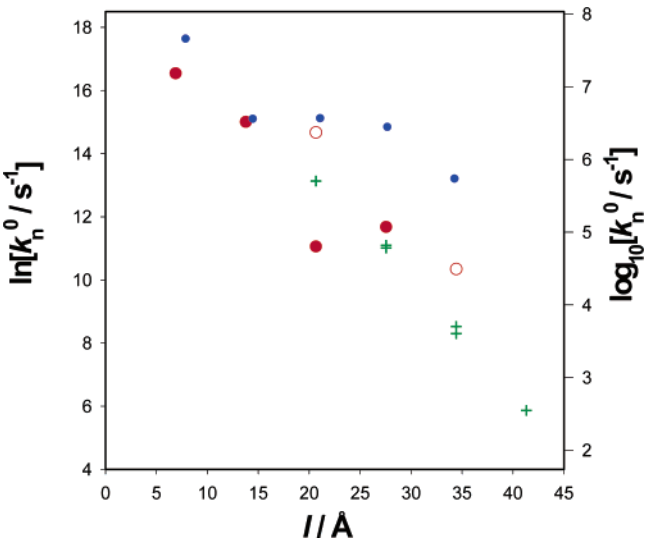

Figure 5. Natural logarithms of all of the standard electron-transfer rate constants (k_n^0) measured at 25 °C in the present study and the study reported in ref 53 versus l. l is defined in footnote *b* of Table 1. Red ○: substituted OPE data measured (using ILIT) in the present study. Red ●: unsubstituted OPE data measured (using ILIT) in the present study. Green +: substituted OPE data measured (using an ac voltammetry technique[69]) in the study reported in ref 53. Blue ●: OPV bridge/ferrocene k_n^0 (for $n = 1-5$) measured[33] at 25 °C plotted as a comparison. The error bars for all of the ILIT data reported in this figure are equal to or smaller than the size of the points (see Table 1).

a number of other experimental differences in the determinations of these standard rate constants between the present study and the study described in ref 53. The most important of these differences are that the ac signals (currents) may be perturbed by the R_uC_{film} time constant associated with any uncompensated solution resistance (R_u) present in the measurements reported in ref 53 and that the concentrations (loadings) of the substituted electroactive compounds in the monolayers investigated in ref 53 were approximately 2 orders of magnitude smaller than the loadings of the electroactive compounds in the monolayers investigated in the present study (see Figure 1). (With respect to the latter difference, the ac-voltammetry data obtained in the study described in ref 53 were relatively insensitive to these small amounts of redox moieties.[70a]) Because ILIT signals are not affected by R_u, because it is difficult to extract accurate values for k_n^0 for systems containing very low loadings (using any technique), and, most importantly, because of the several diagnostic checks we have performed on our ILIT measurements of k_n^0, we will only focus on and discuss the ILIT data obtained with relatively high loadings in the present study. Additionally, as we have noted before,[26] the fact that the standard rate constants measured using ILIT are larger cannot be due to the existence of a heterogeneous distribution of electron-transfer rate constants.[21,30,32,71,72] The observation that the γ values (eqs 3−5) determined by CV and ILIT are the same precludes this possibility.

Arrhenius Analyses of k_n^0 Data. Figure 6 shows Arrhenius plots (eq 1) for all of the electroactive OPE compounds investigated in the present study. The points in all of these plots were obtained at a number of different Γ_T's using mixed monolayers composed of at least two different diluents (except for electroactive compound Vs). The fifth and sixth columns of Table 1 contain the Arrhenius activation energies ($E_{A,n}$, calculated as k_B times the slope of the Arrhenius plot) and the apparent reorganization energy[66] ($\lambda_{n,app}$, calculated using eq 7) determined from the plots in Figure 6. As observed previously at the shortest bridge lengths investigated,[20,26,33] the measured values of $E_{A,n}$ and $\lambda_{n,app}$ for electroactive compound I are considerably smaller than those observed when the bridges of the electroactive compounds were longer. A possible reason for this decrease in $E_{A,n}$ and $\lambda_{n,app}$ at the shortest bridge length (l) studied here will be given later.[73] For unsubstituted bridges containing more than one PE unit, the measured $E_{A,n}$ and $\lambda_{n,app}$ are somewhat larger than those observed with the substituted electroactive compounds (as well as those measured for the electron-transfer reaction of the ferrocene redox moiety through other types of bridges[20,26,33] when the length of the bridge was greater than ~10 Å[74]). However, for the former OPE bridges containing more than one PE unit, any difference in the measured $E_{A,n}$'s for the various bridges investigated here is not significant in comparison to the reported experimental error (see Table 1 and ref 74). Additionally, for (both substituted and unsubstituted) OPE bridges containing two or more PE units, the measured values of $\lambda_{n,app}$ are equivalent to the outer sphere reorganization energies calculated for the interfacial ET reaction of the ferrocene redox couple in aqueous electrolyte solutions.[26]

(70) (a) Bard, A. J.; Faulkner, L. R. *Electrochemical Methods*, 2nd ed.; John Wiley & Sons: New York, 2001; pp 376−387. (b) Bard, A. J.; Faulkner, L. R. *Electrochemical Methods*, 2nd ed.; John Wiley & Sons: New York, 2001; p 102.
(71) Napper, A. M.; Liu, H.; Waldeck, D. H. *J. Phys. Chem. B* **2001**, *105*, 7699−7707.
(72) Tender, L.; Carter, M. T.; Murray, R. W. *Anal. Chem.* **1994**, *66*, 3173−3181.
(73) It should be remembered that the measured standard rate constants for all of the electroactive compounds in Chart 1 are independent of the concentration of the ferrocene redox moiety and the ILIT measured rate constants ($k_m(E_i)$) always exhibit the correct potential dependence (eq 3). The observed decrease in $E_{A,n}$ and $\lambda_{n,app}$ for electroactive compound I, therefore, is not an artifact of our measurements.[2,26]
(74) For these long bridges, the average Arrhenius activation energy for the ferrocene redox couple is ($0.25 \pm 0.01_4$) eV (including the data determined in the present study).[20,26,33]

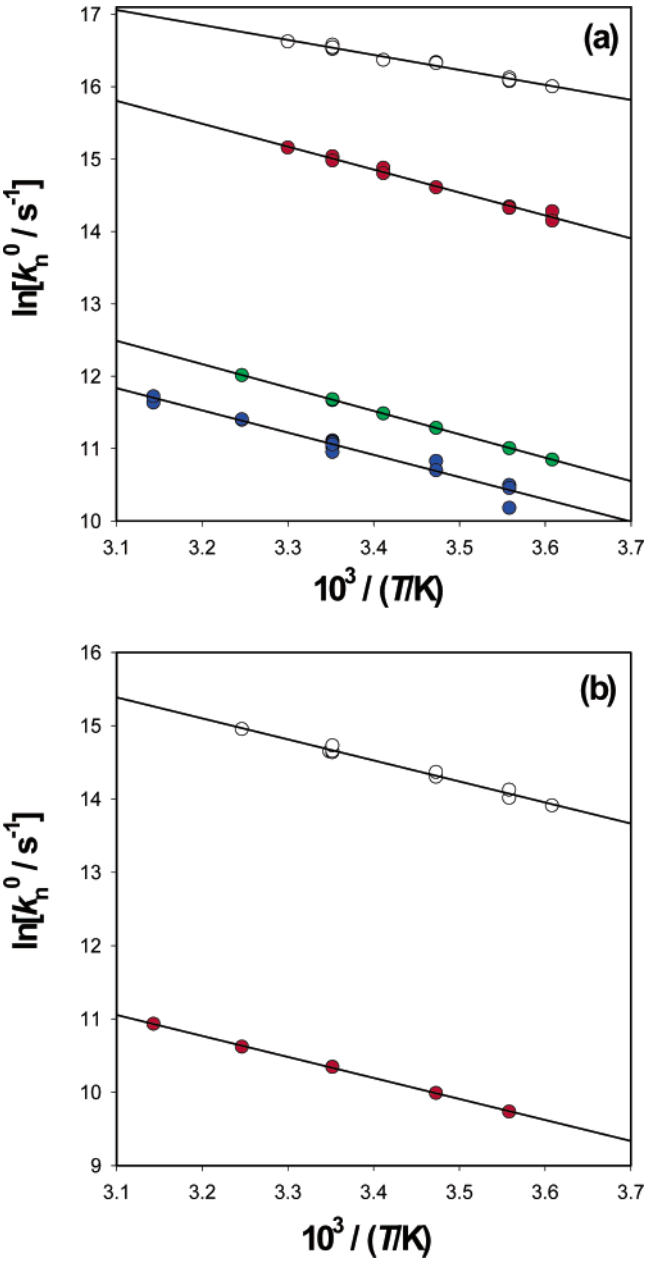

Figure 6. Arrhenius plots. (a) Plots of $\ln[k_n^0]$ vs $1/T$ where the values of k_n^0 are obtained from ILIT experiments on mixed monolayers containing the unsubstituted OPE electroactive compounds and various diluents (see Table 1 and Chart 2). ○: the bridge of the electroactive compound (I in Chart 1) contains one phenyleneethynylene (PE) unit. Red ●: the bridge of the electroactive compound (II in Chart 1) contains two PE units. Blue ●: the bridge of the electroactive compound (III in Chart 1) contains three PE units. Green ●: the bridge of the electroactive compound (IV in Chart 1) contains four PE units. (b) Plots of $\ln[k_n^0]$ vs $1/T$ where the values of k_n^0 are obtained from ILIT experiments on mixed monolayers containing the substituted OPE electroactive compounds and various diluents (see Table 1 and Chart 2). ○: the bridge of the electroactive compound (IIIs in Chart 1) contains three PE units. Red ●: the bridge of the electroactive compound (Vs in Chart 1) contains five PE units. The error bars for all of the data plotted in these figures are equal to or smaller than the size of the points.

(These calculations are modified to take into account the effects (as a function of the thickness of the SAM) of image charges on the solvent reorganization energy[75] and employ the observation[74,76] that the dielectric properties of SAM/electrolyte interfaces are not functions of the thickness of the monolayer.) As we have done before,[26] we conclude from this that the activation entropy of this ET reaction is negligibly small and, most importantly, that the activation energy is solely an attribute of the redox couple (i.e., the OPE bridge does not contribute to $E_{A,n}$).

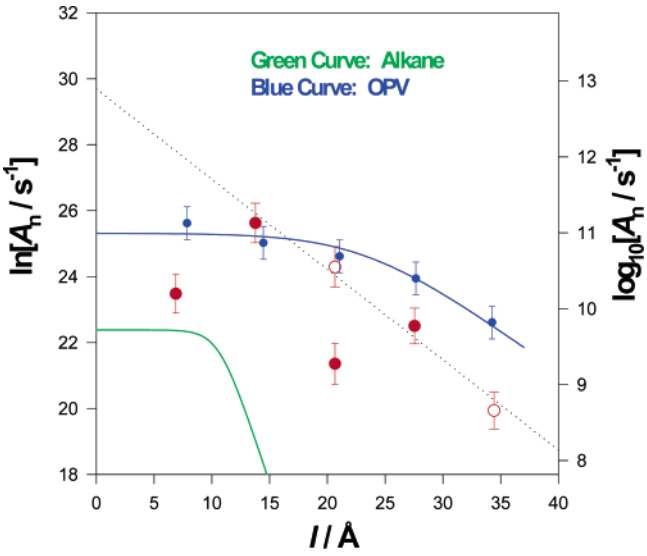

Figure 7. Plots of $\ln[A_n]$ vs l, where A_n is an Arrhenius preexponential factor (see eq 1). Red ●: unsubstituted OPE preexponential factors. Red ○: substituted OPE preexponential factors. The blue points and line describe the data[33] and fitted curve,[26] respectively, for the interfacial electron-transfer reaction of the attached (to Au electrodes) ferrocene redox couple through OPV bridges. The green curve describes the fitted curve[26] for the interfacial electron-transfer reaction of the attached (again, to Au electrodes) ferrocene and (pyridine)$Ru(NH_3)_5^{3+/2+}$ redox couples through alkane bridges. The dotted black line is a linear least-squares fit of an ad hoc subset of the OPE data consisting of the unsubstituted data at $n = 2$ and $n = 4$ as well as the substituted data, resulting in a slope of (-0.27 ± 0.04) Å^{-1} and an intercept of 29.69 ± 0.72.

The seventh column of Table 1 contains the values of $\ln[A_n]$ obtained from the Arrhenius plots in Figure 6. As mentioned in the Introduction, A_n contains information on the factors other than those associated with the reorganization energy of the redox moiety that determine the rate of an interfacial ET reaction (e.g., see eq 6). Because the activation entropy of the interfacial ET reaction that is the subject of the present study is negligible, properties of the OPE bridge determine these factors and, therefore, A_n. The $\ln[A_n]$ values that have been measured for all of the substituted and unsubstituted electroactive compounds listed in Chart 1 are plotted (versus l) in Figure 7. As comparisons, curves representing the behavior of $\ln[A_n]$ for alkane and OPV bridges[26] (as well as the data points for the OPV bridges[33]) are also shown in Figure 7. The most interesting (and important) thing about the OPE data plotted in Figure 7 is that the distance dependence of the unsubstituted OPE data set is not monotonic.[77] This nonmonotonic behavior is very much unlike the weakly distance-dependent, but monotonic behaviors of the alkane (at short bridge lengths) and OPV ($\ln[A_n]$) data sets.[26]

Distance Dependence. Logarithmic plots of both k_n^0 (Figure 5) and A_n (Figure 7) obtained from ILIT measurements with respect to distance l (linearly related to n) display pronounced nonmonotonic behavior. This is true for the homologous subset

(75) Liu, Y.-P.; Newton, M. D. *J. Phys. Chem.* **1994**, *98*, 7162−7169.
(76) Smalley, J. F. *Langmuir* **2003**, *19*, 9284−9289.

(77) This result does not contradict either the observations or the conclusions presented in ref 36.

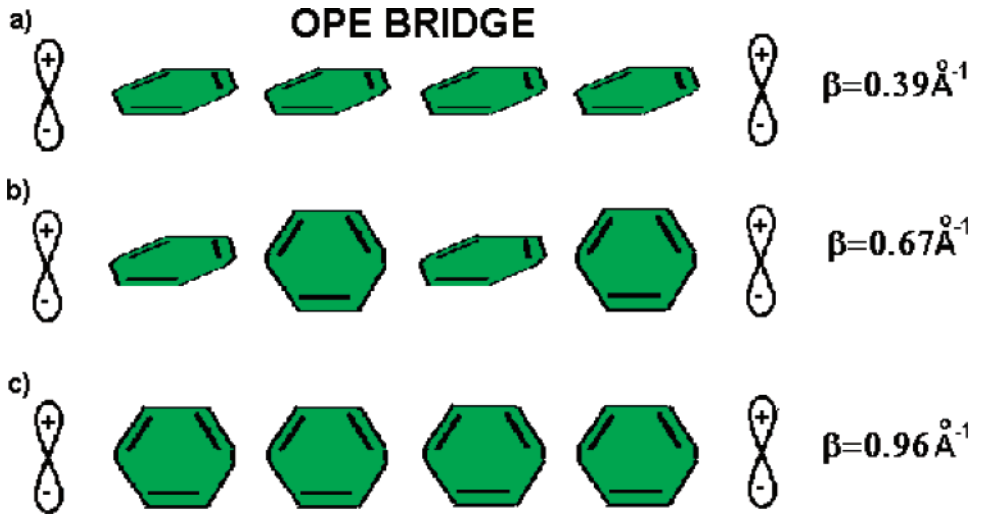

Figure 8. Calculated β values[79] (based on radical cations[79a]) for three torsional variants of the homologous OPE spacer (the schematic representation (shown for a bridge containing four PE units) displays only the phenylene (P) groups and the π orbitals of terminal methylene D and A groups): (a) fully conjugated (all π-planes coincident); (b) successive P π-planes orthogonal, with the D and adjacent P π-planes coincident (the repeat unit for this case is two P moieties); (c) all P planes coincident and orthogonal to the D and A planes. In all cases, the D and A groups are coplanar.

based on unsubstituted OPE's, as well as for the larger set including substituted OPE's. In any case, it is interesting to note that all of the OPE results (to within experimental error) are equal to or less than the envelope provided by the corresponding OPV results, with the separation between OPE and OPV tending to be increasingly pronounced as the oligomers lengthen. This qualitative situation is perhaps not surprising because the OPV oligomers are expected to maintain conformations relatively close to overall framework planarity,[33] whereas larger amplitude conformational fluctuations (i.e., a large amount of torsional disorder in the oligomer backbone[78]) are expected for the OPE systems. If the electronic coupling across a Au/OPV interface is the same as that effected by a Au/OPE interface, the electronic overlap through the OPV oligomers is, thus, more effective than that through their OPE counterparts. A quantitative account of such conformational effects would require a detailed understanding of the intermolecular interactions pertinent to the in situ OPE's, including the manner in which alkyl and alkoxy substituents might affect these interactions.[50,51]

However, molecular orbital calculations have shown the great sensitivity of $H_{ab,n}$ and β values to conformational fluctuations of OPE bridges, with β varying from $\sim$0.3 Å^{-1} for optimally conjugated all-planar OPE's (we adopt this mean value on the basis of the radical cation[79a] results shown in Figure 8 and those given in Table 1 of ref 81, as well as the OPE result given in ref 80) to $\sim$1.0 Å^{-1} for the case in which all phenylene π-manifolds are orthogonal to donor and acceptor π orbitals. (Examples are shown in Figure 8, which displays the results from molecular orbital calculations for three different conformational situations of the (unsubstituted) $n = 4$ oligomer.[79]) As a result of the sensitivity of $H_{ab,n}$ to torsion angle, variation in the distribution of backbone torsion angles (for both the unsubstituted and the substituted OPE series) is likely to be an important contributor to the striking (nonmonotonic) variation of the A_n observed within and between these series. This variation in the distribution of torsion angles does not appear to influence strongly the activation energy,[35,37] although an appreciable entropy contribution may be present. An overall transition state mechanism is proposed here, which involves electron tunneling (as controlled by an equilibrium torsional distribution for a given n value[82]) once the reactant system is thermally activated (as a result of solvent reorganization). According to this proposal, for instance, the seemingly minor substitution of the $n = 3$ OPE backbone (with a single methyl group on the central phenylene) appears to have a major impact on the equilibrium torsional distribution of this backbone.

For the present OPE systems, there is no indication of alternative mechanisms such as torsional gating.[83] While we feel that the n-dependence of A_n for the OPE series is strongly influenced by variation of conformational distribution with n (e.g., as suggested by the great sensitivity of A_n to a methyl group substitution on the central phenylene moiety of $n = 3$ OPE), we note that other factors may play a role, including the occurrence of bond length alternation, which has been invoked in comparison of conductance through OPE and OPV $n = 3$ monolayer junctions.[49,84] As is found for OPE in the present work, in the case of ET through isolated OPV systems,[33] where A_n was found to be unexpectedly flat with respect to l out to nearly 30 Å, the activated process was determined to involve tunneling in the thermally activated ET transition state. However, the rate-determining step controlling A_n (and k_n^0) was attributed to some other dynamical process, thereby implying an overall mechanism beyond the transition state theory framework for OPV bridges. An alternative hopping mechanism through the

(78) Grozema, F. C.; van Duijnen, P. Th.; Berlin, V. A.; Ratner, M. A.; Siebbeles, L. D. A. *J. Phys. Chem. B* **2002**, *106*, 7791−7795.
(79) (a) Newton, M. D. *Int. J. Quantum Chem.* **2000**, *77*, 255−263. (b) Cave, R. J.; Newton, M. D. *J. Chem. Phys.* **1997**, *106*, 9213−9226. (c) Cave, R. J.; Newton, M. D. *Chem. Phys. Lett.* **1996**, *249*, 15−19.
(80) Magoga, M.; Joachim, C. *Phys. Rev. B* **1997**, *56*, 4722−4729.
(81) (a) Newton, M. D. *Theor. Chem. Acc.* **2003**, *110*, 307−321. (b) Newton, M. D. *ACS Symp. Ser.* **2003**, *844*, 196−218.

(82) The observation that γ (see eq 4) is the same no matter whether it is determined using CV or ILIT requires that the entire population of attached redox moieties participates in these equilibria. Additionally, the rates of the forward and reverse reactions in all such equilibria would have to be much faster than the rate of electron transfer, and the observation that the measured $E_{A,n}$ are consistent with Marcus theory requires that the enthalpy changes associated with these equilibria be negligible.[35, 37]
(83) Because $E_{A,n}$ exhibits the expected dependence on n for an activation energy determined by the solvent reorganization energy of ferrocene in water,[26] and $k_m(E_i)$ exhibits the expected (as in Figure 4) dependence on E_i.

OPV bridges was ruled out because hole injection energies were estimated to be at least ~1 eV.[33,85] Hopping has been implicated in some cases of photoinitiated ET though OPV bridges.[86]

Table 1 also reveals that the experimental activation energy $E_{A,n}$ displays a pronounced distance dependence over the $n = 1-5$ range. For a simple nonadiabatic transition state model, $E_{A,n}$ may be expressed as[67]

$$E_{A,n} = \lambda_n/4 - H_{ab,n} \quad (8)$$

Because λ_n in the present case is dominated by solvent reorganization, it is expected[75] to be reduced in magnitude with decreasing l (or n). For a given OPE conformational pattern, the electronic coupling ($H_{ab,n}$) also reduces $E_{A,n}$ with decreasing l. Comparison of $\lambda_n/4$ (based on the model in ref 75 as well as the values of L defined and given in ref 87, together with the static and optical dielectric constants for water) and the experimental $E_{A,n}$ values yields differences of the order of experimental uncertainty (±0.01 eV) except for the $n = 1$ case, where, according to eq 8, we obtain $H_{ab,n} = 0.05$ eV. A direct evaluation of $H_{ab,n}$ for the systems studied experimentally is not possible because of the conformational uncertainties noted above. However, for the purpose of obtaining a rough estimate, if one assumes that the higher lying values of A_n (e.g., for unsubstituted $n = 2$ and $n = 4$, where the measured A_n values are close to the OPV "envelope") correspond to optimal (i.e., near coplanar) OPE conformations, then adopting the standard nonadiabatic model and rearranging eq 6 gives

$$H_{ab,n} = (A_n h/2\pi^{3/2}\rho_m)^{1/2} \quad (9)$$

Together with a value of 0.3 eV^{-1} for the ρ_m of Au[88] and a value of 0.3 $Å^{-1}$ for β,[89] eq 9 yields an estimate of ~0.04 eV for $H_{ab,n}$ where $n = 1$ (unsubstituted OPE), close to the value inferred above from experimental $E_{A,n}$ and calculated l and L values.[87] This calculation suggests that only the fraction of the ferrocene redox couples attached to and coplanar with (see Figure 8) the optimal OPE bridge conformations are reactive,[90] so that, for the short end of the OPE series, $E_{A,n}$ is detectably sensitive to electronic coupling (as expected from eq 8). A similar conclusion was reached previously[26] for ET through alkane-based oligomers.

Electron Transfer through the Diluent. While the electron transfer is generally expected to be dominated by tunneling through the bridge of the electroactive oligomer, the possible role of alternative tunneling pathways involving adjacent diluent oligomers has been a topic of interest.[91] We have previously shown that k_n^0 for ET through OPE thiolates is essentially the same for alkane and OPE diluents,[36] and additional data in Table 1 support this conclusion, thus indicating a minor role for tunneling through diluent oligomers. One might expect a more prominent role for unsaturated diluents (which are capable of better electronic overlap in comparison with saturated systems) when the electroactive oligomers are saturated, as in the case of alkanethiolates. Pertinent to this issue, we note that when $HS(CH_2)_{16}OC(O)Fc$ is the electroactive oligomer, an unsaturated diluent (i.e., diluent 11 in Chart 2) yields 1.2 s^{-1} for k_n^0 (at 25 °C and $n = 16$)), very similar to that observed when a saturated diluent (diluent 6 in Chart 2) is employed ($k_n^0 = 1.4$ s^{-1}).[55] This result indicates that the tunneling is dominated by the electroactive oligomer, even when the latter is saturated and is surrounded by unsaturated diluents.

Conclusions

The ILIT technique has been used to measure the standard rate constants (as a function of temperature) of the ferrocene redox couple attached to Au electrodes through both substituted and unsubstituted OPE bridges that were parts of self-assembled (thiolate) monolayers. The results from Arrhenius analyses of these data demonstrate that the distance dependence of the preexponential factors of the unsubstituted OPE bridges is not monotonic. This observation together with the values and distance-dependent behavior[50,51] of the observed substituted OPE k_n^0 and A_n are consistent with the existence and effects (Figure 8) of the large conformational dispersions expected for OPE bridge/redox couple assemblies. These observations, therefore, provide additional evidence[26,33] suggesting that conformational variability within a bridge (either an equilibrium distribution of conformations as suggested here or some dynamical process associated with the bridge conformations as suggested previously for alkane[26] or OPV[33] bridges) can have a significant impact on the kinetics of an interfacial electron-transfer reaction through the bridge.[86]

Two additional conclusions may be drawn from the observations obtained in the present study. First, the observed rate of

(84) An interesting comparison[49a] of conductance (g) in molecular junctions based on $n = 3$ neat OPV and OPE dithiolate films linked to gold electrodes has found the conductance of OPV to be uniformly greater than that for OPE over biases ranging from 0 to 1 V. Furthermore, DFT and Green function calculations for the conductance through single-molecule junctions in which the OPE and OPV spacers are constrained to be planar (and thus with optimal torsion angles for both spacers), and for a bias of 0.5 V, yielded g(OPV) > g(OPE) by a factor of 8.[49a] It was noted that the greater bond length alternation between phenylene and ethynylene moieties as compared to that for phenylene and vinylene moieties might be a significant factor in accounting for larger spacer band gaps and hence reduced g. However, we note that the difference in the length of single bonds in OPE and OPV tends to reduce the overall pattern of bond length alternation in these systems. We also note that INDO/s CI calculations (of the type reported in refs 79a and 81) for planar unsubstituted $n = 3$ OPE and OPV systems yield similar values for the band gap (~3.5 eV) and $H_{ab,n}$ (within ~25%), whereas torsional dispersion (using either a random distribution or one based on the small rotational barrier (~k_BT at 300 K) in a PE unit) leads to a pronounced reduction in $H_{ab,n}$ for OPE (by a factor of 3 for $n = 3$),[81] in contrast to a relatively minor effect on OPV. The presence of alkoxy groups on the phenylene moieties in the planar OPV spacers is known[81b, 86b] to reduce the ionization potential and red shift the band gap relative to unsubstituted OPV (e.g., INDO/s CI calculations yield a red shift of 0.3 eV for 2,5-dimethoxy substitution of the central phenylene group in $n = 3$ OPV), but the influence on $H_{ab,n}$ (a reduction of less than 10% for $n = 3$) and β was found to be minor.[81]

(85) Sikes, H. D.; Sun, Y.; Dudek, S. P.; Chidsey, C. E. D.; Pianetta, P. *J. Phys. Chem. B* **2003**, *107*, 1170−1173.

(86) (a) Davis, W. G.; Ratner, M. A.; Wasielewski, M. R. *J. Am. Chem. Soc.* **2001**, *123*, 7877−7886. (b) See also: Davis, W. G.; Wasielewski, M. R.; Ratner, M. A. *Int. J. Quantum Chem.* **1999**, *72*, 463−471.

(87) According to the theory described in ref 75, λ_n is a function of the quantity L (essentially the thickness of the monolayer) rather than l (but L is nearly linearly related to l). For $HS(CH_2)_nCH_3$ (diluents 4, 6, and 10 in Chart 2), $L = 2.10$ Å + 1.09 Å$(n + 1)$; for $HS(CH_2)_nOH$ (diluents 1, 3, and 7 in Chart 2), $L = 4.06$ Å + 1.09 Å(n); for diluent number 8 in Chart 2, $L = 21.63$ Å; for diluent number 2 in Chart 2, $L = 6.85$ Å; for diluents numbers 5 and 11 in Chart 2, $L = 11.78$ and 18.67 Å, respectively; and for diluent number 9 in Chart 2, $L = 20.70$ Å (average of the values for diluents numbers 6 and 7). Note that all of these values of L include the diameter of the adsorbed sulfur atom.

(88) Royea, W. J.; Fajardo, A. M.; Lewis, N. S. *J. Phys. Chem. B* **1997**, *101*, 11152−11159.

(89) We note that a value of $\beta \approx 0.3$ $Å^{-1}$ is also obtained from a fit to a subset of the OPE A_n versus l data that includes the unsubstituted data at $n = 2$ and $n = 4$ as well as the substituted data (see the black dotted line in Figure 7). However, the choice of such a subset is ad hoc and unnecessary for the present rough calculation.

(90) For example, all of the other (nonreactive) conformations could be in equilibrium with the reactive, optimal conformations.[82]

(91) Slowinski, K.; Chamberlain, R. V.; Miller, C. J.; Majda, M. *J. Am. Chem. Soc.* **1997**, *119*, 11910−11919.

electron transfer for a particular OPE bridge is independent of the chemical identity of the diluent component in the mixed monolayer used to determine this rate, and employing an unsaturated OPE diluent in the mixed monolayer has no effect on the rate of electron transfer through a long-chain alkanethiol bridge (i.e., the k^0 measured for $HS(CH_2)_{16}OC(O)Fc$). These observations suggest that the tunneling pathway is confined to the electroactive thiolate, which, thereby, rules out participation of the surrounding unsaturated diluent molecules in the tunneling. Second, the observation that the measured A_n is independent of the terminal functional group of the diluent demonstrates that the rate of electron transfer (and, therefore, the electrical resistance of the bridge; see below) is independent of the potential drop through the monolayer.[92]

Understanding the physical and chemical factors that control electron conduction through individual molecules is critically important for the design and construction of molecular electronic devices.[12] We have discussed[26] an approximate relationship between the Arrhenius preexponential factor measured for a specific metallic electrode−bridge−redox couple structure and the electrical resistance (R_m) of the bridge[70b]

$$R_m = \frac{2k_B T}{A_n e^2} \tag{10}$$

R_m is a function of A_n (and not k_n^0) because the reorganization energy of the redox couple does not influence the electronic conduction through the bridge.[95] (Each conductance determined in the measurements described in refs 45, 52, 97, and 99 (see below) was assumed not to be activated.) Values of R_m estimated using eq 10 turn out to be quite similar[13] to those based on a theory of Nitzan (which pays explicit attention to the relevant densities of states governing the conductance and the activated ET kinetics).[95] As examples,[96] from eq 10 and the A_n data in Table 1, the OPE bridges for electroactive compounds II and III exhibit resistances (at 300 K) of 2.4×10^6 and 1.7×10^8 Ω, respectively. These estimated resistances compare quite well with the resistances (near zero bias[96]) that have recently been reported for molecular junctions composed of individual 4,4′-bipyridine molecules[97] ($(1.3 \pm 0.1) \times 10^6$ Ω) and individual 1-nitro-2,5-di(phenylethynyl-4′-mercapto)benzene molecules (2×10^8 Ω),[52,98] respectively. On the other hand, the resistances calculated for both compound II and compound III are orders of magnitude less than the $(5.2 \pm 1.8) \times 10^{10}$ Ω resistance that has recently been measured[45,99] (at low bias[96]) for the 2,5-di-(phenylethynyl-4′-thioacetyl) benzene (TPE-dithiol) single-molecule nanojunction using conducting atomic force microscopy (AFM). We should point out that the disagreement between the single-molecule resistances estimated (employing ILIT results) for the bridges of compounds II and III and that determined (using an AFM technique) for TPE-dithiol may simply be due to the different molecular structures investigated, which also means that the agreement between the R_m estimated above for compounds II and III and those reported for 4,4′-bipyridine and 1-nitro-2,5-di(phenylethynyl-4′-mercapto)benzene (respectively) should be interpreted with caution. However, the large differences[26] between the single-molecule resistances determined using ILIT and the AFM technique may also be a consequence of a contact resistance[100] between the AFM probe and the Au nanoparticle ("contact pad") employed in the latter technique[99] or other physical dissimilarities between the junctions investigated in the present study and in refs 45 and 99.

The ILIT technique is, nevertheless, a robust and highly reproducible technique for the estimation of the conductance through individual molecular bridges as well as for the study of the physical and chemical factors that define the mechanism of electron transport through these bridges. In regard to these factors, clearly, a full understanding of ET kinetics and conductance through both OPV and OPE bridges, including the nonmonotonic behavior of A_n for OPE and the great apparent sensitivity of a given OPE bridge ($n = 3$) to the presence of a methyl substituent on the central phenylene moiety, warrants further detailed study, both experimental and theoretical.

Acknowledgment. J.F.S., S.W.F., and M.D.N. gratefully acknowledge the support of the U.S. Department of Energy, Contract No. DE-AC02-98CH10886. C.E.D.C., S.B.S., S.P.D., and H.D.S. thank the National Science Foundation for support (Grants CHE-9412720 and CHE-961212725). S.E.C. also thanks the National Science Foundation for support (Grant CHE-9616370). Discussions with and suggestions from Dr. Jack Fajer (Materials Science Department, Brookhaven National Laboratory) are also gratefully acknowledged.

JA047458B

(92) Because the mole fraction of the electroactive compound in the SAMs investigated in the present study is always less than 0.10, the potential drop through the monolayer at the $E^{\circ\prime}$ of the redox couple (ΔV_M) may be defined as ($E^{\circ\prime} - E_{pzc}$), where E_{pzc} is the potential of zero charge of a Au electrode coated with a neat SAM of the diluent. (According to this definition, ΔV_M is the difference in potential between the electrode and the electrolyte solution at the high ionic strengths used in the present study.) The potentials of zero charge (versus SSCE) of Au electrodes coated with monolayers composed of simple alkanethiols, ω-hydroxy alkanethiols, and ω-mercaptoalkanoic acids are (approximately) −0.40,[93] −0.07,[93] and 0.08 V,[76] respectively. For electroactive compound III then, measurements of the rate of electron transfer took place when $\Delta V_M = 0.75$, 0.41, and 0.24 V, respectively. The good fits to eqs 3−5 (such as those shown in Figure 4) also demonstrate that changing the potential drop through the monolayer by as much as an additional ±0.15 V has no effect on the rate of electron transfer through OPE bridges. However, the distributions of electrostatic potential along the lengths of these bridges are unknown.[13,33,94]

(93) Becka, A. M.; Miller, C. J. *J. Phys. Chem.* **1993**, *97*, 6233−6239.
(94) Mujica, V.; Roitberg, A. E.; Ratner, M. *J. Chem. Phys.* **2000**, *112*, 6834−6839.
(95) Nitzan, A. *J. Phys. Chem. A* **2001**, *105*, 2677−2679.
(96) We should emphasize that, even though there are significant potential changes across the Au-bridge-Fc junctions effected by the SAMs employed in the present study,[92] the electron-transfer reaction in an ILIT experiment is driven by a free energy change that is always less than a few millielectronvolts (see, for example, the data in Figures 2 and 3).
(97) Xu, B.; Tao, N. J. *Science* **2003**, *301*, 1221−1223.
(98) A calculated[52] conductance based upon the model presented in ref 13 also is in excellent agreement with the measured conductance reported in ref 52. However, we should point out that the authors of ref 52 assume that their measured conductance is effected by a "hopping" mechanism while the model presented in ref 13 is a only valid for a (nonresonant) tunneling mechanism.
(99) Ramachandran, G. K.; Tomfohr, J. K.; Li, J.; Sankey, O. F.; Zarate, X.; Primak, A.; Terazono, Y.; Moore, T. A.; Moore, A. L.; Gust, D.; Nagahara, L. A.; Lindsay, S. M. *J. Phys. Chem. B* **2003**, *107*, 6162−6169.
(100) Lang, N. D.; Avouris, Ph. *Phys. Rev. B* **2001**, *64*, 125323.